

# Van der Waals Density Functional for Layered Structures

H. Rydberg,<sup>1</sup> M. Dion,<sup>2</sup> N. Jacobson,<sup>1</sup> E. Schröder,<sup>1</sup>  
 P. Hyldgaard,<sup>1</sup> S.I. Simak,<sup>1</sup> D.C. Langreth,<sup>2</sup> and B.I. Lundqvist<sup>1,\*</sup>

<sup>1</sup>*Department of Applied Physics, Chalmers University of Technology and Göteborg University, SE-412 96 Göteborg, Sweden*

<sup>2</sup>*Center for Materials Theory, Department of Physics and Astronomy,  
 Rutgers University, Piscataway, New Jersey 08854-8019*

(Dated: May 31, 2003)

Understanding of biostructures, soft matter, and other abundant sparse systems calls for accounts of both strong local atom bonds and weak nonlocal van der Waals forces between atoms separated by empty space. A fully nonlocal version of the functional form [H. Rydberg, B.I. Lundqvist, D.C. Langreth, and M. Dion, Phys. Rev. B **62**, 6997 (2000)] of density-functional theory (DFT) is applied here to the layered systems graphite, boron nitride, and molybdenum sulfide to compute bond lengths, binding energies, compressibilities, and other properties of soft bonds. These key examples show that the DFT with the generalized-gradient approximation does not apply for calculating properties of sparse matter, while use of the fully nonlocal version appears to be one way to proceed.

PACS numbers: 71.15.Mb, 61.50.Lt, 31.15.Ew, 73.21.-b

Calculations of structure and other properties of sparse systems must account for *both* strong local atom bonds *and* weak nonlocal van der Waals (vdW) forces between atoms separated by empty space. Present methods are unable to describe the true interactions of sparse systems, abundant among materials and molecules. Key systems like graphite, BN, and MoS<sub>2</sub> have layered structures. They are important for various technologies, *e.g.*, lubrication, nanotechnology, and catalysis. While today's standard tool, density-functional theory (DFT), has achieved impressive application breadth, the common local (LDA) and semilocal density approximations (GGA) [1, 2, 3, 4] for exchange and correlation,  $E_{xc}[n]$ , fail to describe the interactions at sparse electron densities. Here we show that the recently proposed density functional [5] with nonlocal correlations,  $E_c^{nl}[n]$ , gives separations, binding energies, and compressibilities of these layered systems in fair agreement with available experimental data. This planar case gives us experience with a strong bearing on vdW density functionals for general geometries [6, 7], as do asymptotic vdW functionals [8], and provides tests and clues for this development work.

Figure 1 with its 'inner surfaces' defines the problem: voids of ultra-low density, across which electrodynamics leads to vdW coupling. This coupling depends on the polarization properties of the layers themselves, and *not* on small regions of density overlap between the layers, giving no chance for proper account in LDA or GGA, which are totally dependent on the overlap region. For large interplanar separation  $d$  the vdW interaction energy between planes behaves as  $-c_4/d^4$ , while LDA or GGA necessarily predicts an exponential falloff. Layers rolled up to form two (i) nanotubes with parallel axes a distance  $l$  apart interact as  $-c_5/l^5$ , or (ii) balls (*e.g.*, C<sub>60</sub>), a distance  $r$  apart, as  $-c_6/r^6$ . If by fluke an LDA or GGA were to give the correct equilibrium for one shape, it would necessarily fail for the others. The simple ex-

pedient of adding the standard asymptotic vdW energies as corrections to the correlation energy of LDA or GGA also fails. The true vdW interaction between two close sheets must be substantially stronger (Fig. 1). It must also be *seamless*, and saturate as  $d$  goes to zero (Fig. 2).

Like earlier work directly calculating nonlocal correlations between two jellium slabs [9], the vdW density functional (vdW-DF) theory [5] used here exploits assumed planar symmetry. It divides the correlation energy functional into two pieces,  $E_c[n] = E_c^0[n] + E_c^{nl}[n]$ , where  $E_c^{nl}[n]$  is defined to include the longest ranged or most nonlocal terms that give the vdW interaction and to approach zero in the limit of a slowly varying density. The term  $E_c^0[n]$  is also nonlocal, but approaches the LDA in this limit. The two terms are approximated differently. In particular, we make the LDA for  $E_c^0[n]$ , arguing that after separating off the principal longest range terms, the LDA will be much more accurate. Ultimately we may propose gradient corrections to  $E_c^0[n]$ , but these are expected to be small. So in this work we use

$$E_c[n] \approx E_c^{\text{LDA}}[n] + E_c^{nl}[n]. \quad (1)$$

Long range terms are less sensitive to details of the system's dielectric response than the short range terms. Thus very simple approximations for the dielectric function are made for  $E_c^{nl}[n]$ . The principal requirement is that the polarization properties of a single layer come out reasonably, and we take care to make sure this is so.

For systems with planar symmetry, the predominant component of the nonlocal correlation energy  $E_c^{nl}$  giving the vdW forces can be determined simply by comparing the solutions of the Poisson equation  $\nabla \cdot (\epsilon \nabla \Phi) = 0$  and the Laplace equation  $\nabla^2 \Phi = 0$  [5]. The crux of the approximation is the use of a simple plasmon-pole model for the dielectric function,

$$\epsilon_k(z, iu) = 1 + \frac{\omega_p^2(z)}{u^2 + (v_F(z)q_k)^2/3 + q_k^4/4}, \quad (2)$$

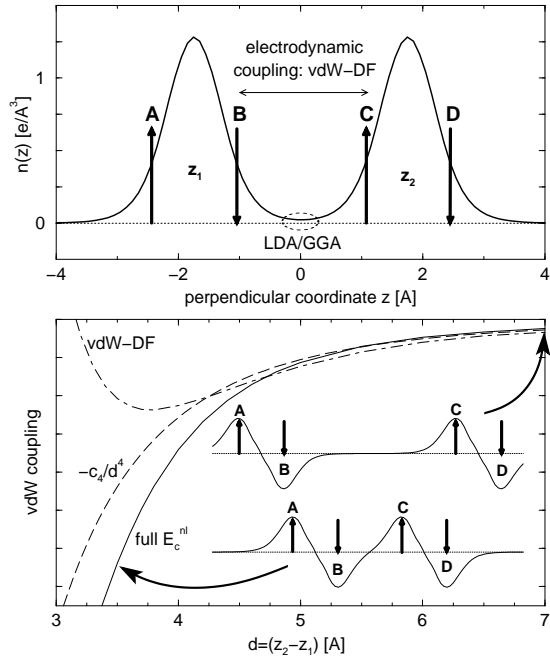


FIG. 1: Schematics of the vdW forces in sparse, layered materials. *Top panel*: Laterally averaged electron-density profile of two graphene layers at equilibrium separation  $d \approx 3.5 \text{ \AA}$ . The dotted ellipse indicates the density region that determines the interlayer interaction within LDA or GGA. It cannot describe the true long range interaction (horizontal arrow) between correlated charge fluctuations, whose extrema are illustrated by those of the finite-frequency charge response, and labelled by vertical arrows. *Bottom panel*: Full  $E_c^{\text{nl}}$  (solid curve) vs. the asymptotic form of  $E_c^{\text{nl}} \rightarrow -c_4/d^4$  (dashed line). Also shown: full ground state interaction energy (dash-dotted line). *Insets*: Sketches of the correlated charge fluctuations for different layer separations, explaining why  $|E_c^{\text{nl}}| > c_4/d^4$  (by  $\sim 50\%$  near equilibrium). In the asymptotic region (top inset), attractive interactions BC and AD are nearly cancelled by the repulsive interactions AC and BD, leaving little more than the weak dipolar interaction. Near equilibrium separation (bottom inset), the repulsive interactions AC and BD remain specified by the layer separation  $d$ , but the relative strengthening of attractive interaction BC substantially overcompensates the relative weakening of the attractive interaction AD. At still smaller  $d$ ,  $E_c^{\text{nl}}$  becomes weaker and saturates (Fig. 2, inset).

where  $\omega_p^2(z) = 4\pi n(z)e^2/m$ , and  $mv_F(z) = (3\pi^2 n(z))^{1/3}$  are functions of the local density  $n(z)$ . The wave vector perpendicular to the  $z$  direction is  $\mathbf{k}$ , and  $iu$  is the imaginary frequency. The quantity  $q_k$ , given by  $q_k^2 = k^2 + q_\perp^2$ , is used to mimick the three-dimensional wave vector. The  $z$  direction is accounted for already by the  $n(z)$  dependence, and  $q_\perp$  is just taken to be a constant.

Our scheme, applied to jellium surfaces in Ref. 5, is used here for layered systems. For simplicity, consider a two-layered system (*e.g.*, two parallel graphene sheets) arranged perpendicular to the  $z$  axis, at positions  $z = 0$  and  $z = d$ , respectively. The first step is to calculate the

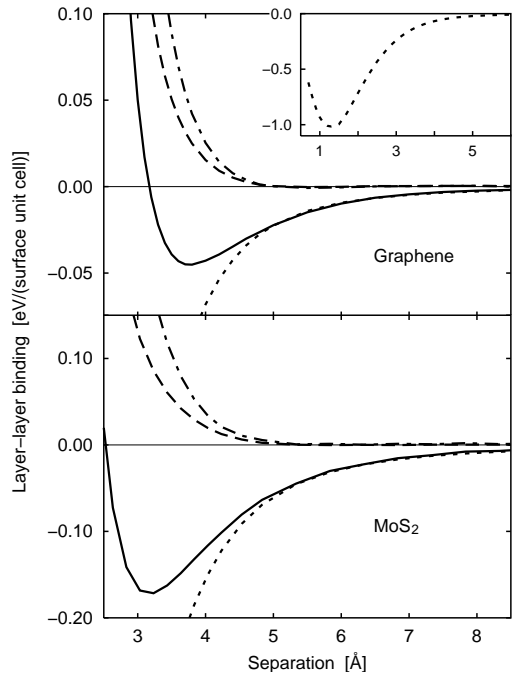


FIG. 2: Calculated vdW-DF results for the interlayer binding (adhesion) between two sheets of graphene (*upper panel*) and MoS<sub>2</sub> (*lower panel*) as functions of the interlayer separation  $d$ . The panels each compare the variation in the vdW-DF adhesion energy (solid curves) with that of the underlying GGA (dashed curves), and with the adhesion *in the absence of* the vdW-DF term  $E_c^{\text{nl}}$  (dash-dotted curves) calculated using only the first two terms of Eq. (5) for  $E_{\text{xc}}$ . The nonlocal-correlation vdW contribution  $E_c^{\text{nl}}$  alone is shown separately (dotted curves). The figure shows that no binding results from exchange or local correlation; the vdW interactions provides adhesion in fair agreement with experiment (Table I). The *inset* shows that our calculated value of  $E_c^{\text{nl}}$  saturates for small  $d$  values.

density in DFT with a suitable approximation, which we take to be an appropriate flavor of the GGA, and to average it in the lateral direction to yield  $n(z)$ . The next two steps represent the key to the success of our approximation. First one calculates from first principles the perpendicular static polarizability  $\alpha$  of a *single* layer of the material (a graphene layer in this example) in the ground-state DFT scheme with the above GGA flavor. Then one fixes the constant  $q_\perp$  so that dielectric model (2) gives precisely the same polarizability, that is to say

$$\alpha = \frac{1}{4\pi} \int dz \left[ 1 - \frac{1}{\epsilon_0(z, 0)} \right]. \quad (3)$$

This step mitigates the errors introduced both by the lateral averaging and the dielectric model. The leading vdW interaction is proportional to an integral over the square of the dynamic polarizabilities. Previous work in the asymptotic limit [8] shows that simple, properly scaled dielectric functions giving the correct static po-

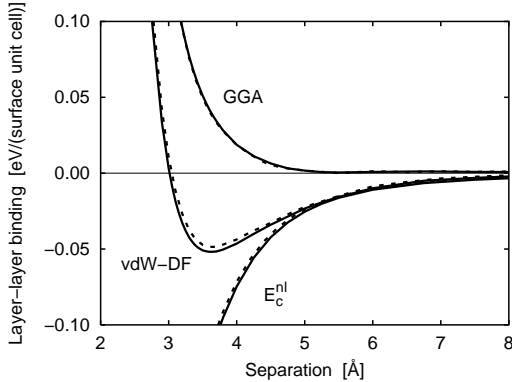


FIG. 3: Comparison of the vdW-DF layer-to-layer binding in the staggered bulk hexagonal-BN system (solid lines) and adhesion between two sheets of BN (broken lines) shown as functions of the interlayer separation  $d = c/2$ . In both descriptions the GGA gives unphysical results for bond and equilibrium separation. The total adhesion is dominated by the contribution of the vdW interaction  $E_c^{nl}$ . The figure emphasizes that the nearest-neighbor interlayer binding (broken lines) strongly dominates the bulk adhesion (solid lines) for layered materials.

larizabilities form good approximations to the dynamic ones, and hence give accurate vdW interactions.

The correlation energy of an arbitrary system can be calculated once the system response to all possible (hypothetical) external charge distributions is known [10]. With planar symmetry only the response to an arbitrarily charged sheet placed at an offset from one end of the sample needs to be calculated:  $\rho \propto \exp(i\mathbf{k} \cdot \mathbf{r})\delta(z - z_-)$ , where  $z_- \ll 0$ . Integrating Poisson's equation with  $\epsilon$  as in (2) one finds the  $z$  component of the electric field  $E_z(z_+)$  at  $z = z_+ \gg d$ . Then  $E_c^{nl}$  is given by [5]

$$E_c^{nl} = -A \int_0^\infty \frac{du}{2\pi} \int \frac{d^2k}{(2\pi)^2} \ln \frac{E_z(z_+)}{E_z^0(z_+)}, \quad (4)$$

where  $A$  is the lateral area and  $E_z^0(z_+)$  is the electric field component produced by the charge sheet at  $z = z_-$  in the absence of the sample. In Eq. (4) the spatial dependences of the two  $E$ 's cancel in the ratio, leaving only the  $k$  dependence. We used the obvious extension of this method to 32 and 30 layers slabs to give, by subtraction, a well converged per layer value of  $E_c^{nl}$  for each of the bulk solids considered here.

The approximation for the exchange energy functional  $E_x[n]$  should be consistent with our approximation for  $E_c^0[n]$ , that is a local or semilocal one. We use a version that best approximates exact density functional exchange, namely Zhang and Yang's [3] (ZY) "revPBE" exchange functional  $E_x^{ZY}[n]$ , where the parameter controlling the large gradient limit in the PBE exchange functional [2] is fitted to exact density-functional exchange calculations. Unlike exchange [11] in PW91 [1], PBE [2], and RPBE [4],  $E_x^{ZY}$  shows no tendency to bind any of

TABLE I: Properties of graphite, BN, and MoS<sub>2</sub>, calculated with vdW-DF and compared to experimental data in parentheses, when available. The table shows the geometry ( $a, c$ ), binding energy ( $E_0$ ), bulk modulus ( $B_0$ ), and elastic constant ( $C_{33}$ ). GGA (not shown) binds very weakly at unphysically large  $c$  or not at all, depending on substance and GGA flavor.

	Graphite	BN	MoS <sub>2</sub>
$a$ [Å]	2.47 (2.46) <sup>a</sup>	2.51 (2.50) <sup>b</sup>	3.23 (3.160) <sup>c</sup>
$c$ [Å]	7.52 (6.70) <sup>d</sup>	7.26 (6.66) <sup>b</sup>	12.6 (12.29) <sup>c</sup>
$E_0$ [meV/at]	24 (35 $\pm$ 10) <sup>e</sup>	26	60
$B_0$ [GPa]	12 ( $\sim$ 33) <sup>a</sup>	11	39
$C_{33}$ [GPa]	13 (37-41) <sup>a</sup>	11	49

<sup>a</sup>Ref. 23.

<sup>b</sup>Ref. 24.

<sup>c</sup>Ref. 25.

<sup>d</sup>Ref. 26.

<sup>e</sup>Ref. 27.

the vdW systems we have tried it on, unless the vdW correlation is actually included in the calculation. We thus take

$$E_{xc}[n] = E_x^{ZY}[n] + E_c^{LDA}[n] + E_c^{nl}[n]. \quad (5)$$

The first two terms form an important and recommended starting point for testing nonlocal vdW functionals. They assure a vdW attraction that actually comes from terms that are capable in principle of giving it.

In order to preserve the use of GGA to calculate densities of individual layers, we implement the above scheme by calculating the energy  $E^{GGA}$  and density  $n^{GGA}$ , typically in the revPBE flavor of GGA. The total energy, as a function of the lattice parameters, is then calculated as  $E \approx E^{GGA}[n^{GGA}] + \Delta[n^{GGA}]$ , where  $\Delta[n] = E_c^{nl}[n] - E_c^{\text{grad}}[n]$ ,  $E_c^{\text{grad}}[n]$  being the part of the GGA correlation functional that depends on density gradients,  $E_c^{\text{grad}}[n] = E_c^{GGA}[n] - E_c^{\text{LDA}}[n]$ . This approximation treats  $\Delta$  as a post GGA perturbation and thus neglects the influence of the vdW interaction on the density. The GGA calculations are done using the plane-wave pseudopotential [12] DFT code dacapo [13].

The three materials considered here have layered structures with a soft direction perpendicular to the layers [14]. Strong covalent bonds occur between the atoms within the hexagonal layers (lattice constant  $a$ ), having staggered or A-B type stacking. Graphite is a textbook example of a system with interplanar vdW interactions, with the intralayer C atoms in regular, planar hexagons stacked with hexagon corners on top of hexagon centers. Boron nitride, isoelectronic with graphite, has no shift in hexagon locations but B and N atoms in alternate positions along the  $c$ -direction. A similar alternation between Mo and S atoms occurs in the experimentally relevant A-B type structure of MoS<sub>2</sub> [15].

Calculations are also performed for bilayers of the

three systems. The binding-energy curve of two parallel graphene sheets [16], *i.e.*, the total-energy difference at separation  $d$  and at infinite separation, respectively, for varying  $d$  (Fig. 2) gives in the approximation [5] with vdW-DF, Eq. (5), a close relation to experimental findings for binding energy and equilibrium distance. The GGA curve, on the other hand, is completely wrong, which we blame on absence of vdW effects. The inset shows that our  $E_c^{\text{nl}}$  contribution gives rise to stronger binding than the traditional asymptotic vdW interaction at relevant separations. The binding-energy curve for two parallel BN sheets (Fig. 3) differs little from that of bulk BN as a function of lattice constant  $c$ . At equilibrium the calculated  $E_c^{\text{nl}}$  difference is  $\sim 4\%$ , attributable mostly to 2nd nearest layers in the bulk material [17].

Compressibility is the epitome of softness, and so bulk-modulus values are computed together with other structure ( $a, c$ ) and bonding properties [18] (Table I). It is crucial to densely sample the region of  $(a, c)$  values around the optimal structure  $(a_0, c_0)$ , and we use a new method [19] for direct evaluation of both structure, binding energy, and bulk modulus  $B_0$  with about 150 points in the relevant range of  $a$  and  $c$  values [20]. GGA values were also computed but not shown. For all three materials the GGA (revPBE flavor) gives no binding or binds very weakly at unreasonably large separation, as do other GGA flavors. The vdW-DF, on the other hand, gives values for lattice parameters and cohesive energy in good agreement and for bulk modulus in fair agreement with experimental values, when available. The BN results come out very close to those of graphite. The results for the A-B type MoS<sub>2</sub> are in very good agreement with experiment.

In conclusion, we recommend the replacement of GGA as a standard method in total-energy calculations with vdW-DF as given in Eq. (5) for descriptions of layered systems that contain sparse electron distributions. This will give the right qualitative character of soft bonds, including saturation of the vdW potential at small separations, and even quantitative ones, like physical values of bond lengths, binding energies, and compressibilities.

We are grateful to K. W. Jacobsen for directing our attention to the problem of the vdW binding of MoS<sub>2</sub> layers [21]. Financial support from the Swedish Foundation for Strategic Research via Materials Consortia #9 and ATOMICS and the Swedish Scientific Council are gratefully acknowledged. Work by M.D. and D.C.L. supported in part by NSF Grant DMR 00-93070.

- [2] J. P. Perdew, K. Burke, and M. Ernzerhof, Phys. Rev. Lett. **77**, 3865 (1996).
- [3] Y. Zhang and W. Yang, Phys. Rev. Lett. **80**, 890 (1998).
- [4] B. Hammer, L. B. Hansen, and J. K. Nørskov, Phys. Rev. B **59**, 7413 (1999).
- [5] H. Rydberg, B. I. Lundqvist, D. C. Langreth, M. Dion, Phys. Rev. B **62**, 6997 (2000).
- [6] H. Rydberg, Ph D. Thesis (2001), Chalmers University of Technology, ISBN 91-7291-068-2.
- [7] M. Dion, H. Rydberg, B. I. Lundqvist, and D. C. Langreth, to be published.
- [8] See E. Hult, P. Hyldgaard, J. Rossmeisl, and B. I. Lundqvist, Phys. Rev. B **64**, 195414 (2001) and E. Hult, H. Rydberg, B. I. Lundqvist, D. C. Langreth, Phys. Rev. B **59**, 4708 (1998), and references therein.
- [9] J. F. Dobson and J. Wang, Phys. Rev. Lett. **82**, 2123 (1999).
- [10] The coupling constant integration in  $E^{\text{nl}}$  is performed via the following approximation:  $\epsilon - 1 \approx \lambda[(\epsilon - 1)/\lambda]_{\lambda=1}$ . This approximation gives the long range van der Waals interaction exactly [7] for dielectric functions of the type used here. The  $\lambda$  dependence comes via  $q_{\perp}$ .
- [11] Y. Zhang, W. Pan, and Y. Yang, J. Chem. Phys. **107**, 7921 (1997); X. Wu et al., J. Chem. Phys. **115**, 8748 (2001).
- [12] Typically core excitations have large energy denominators and hence do not make large contributions to the polarizability or vdW interactions. This has been respected by previous functionals [8] and presumably in principle by this one also. However, lateral averaging has a perverse effect on how core states appear to the functional. By substantially increasing their volume, and reducing their density, they might appear more like valence states to the functional. Despite this, in explicit testing on graphene we have found their effect on equilibrium geometries to be negligible, while giving a  $\sim 30\%$  increase in well-depth. Believing these small effects to be spurious, we did not include core contributions to the density.
- [13] L. B. Hansen et al., computer code DACAPO, The Center for Atomic-Scale Materials Physics (CAMP), Technical University of Denmark, Lyngby, Denmark, using well-converged samplings of k-points and energy-cutoff values.
- [14] Separation  $d = c/2$ , except for MoS<sub>2</sub>, where  $d$  is defined as the distance from the perpendicular position of the top-most sulfur atom of one layer to the position of the bottom-most sulfur atom of the next.
- [15] In the MoS<sub>2</sub> interlayer calculations, each MoS<sub>2</sub> layer is treated as a composite material (the Mo-S perpendicular separation is  $\sim 1.58$  Å). A composite  $q_{\perp}$  value ( $\sim 0.58$ ), identical in both MoS<sub>2</sub> layers, is obtained by applying an external field across a single MoS<sub>2</sub> composite and using GGA to calculate the static polarization. In the interaction study the vdW-DF energy is then calculated as a function of the separation between the two MoS<sub>2</sub>-layer composite materials, the atom positions within each of the MoS<sub>2</sub>-layer composites being kept fixed.
- [16] M. S. Dresselhaus, G. Dresselhaus, K. Surihara, I. L. Spain, H. A. Goldberg, *Graphite Fibers and Filaments* (Springer, Berlin, 1988).
- [17] The 4% figure may be estimated as  $1/(1.5 \times 2^4)$ , with the divisor of 1.5 occurring because the 50% enhancement (Fig. 1) is not applicable at the 2nd layer distance.
- [18] Using  $E_{\text{vdW-DF}}(c, a) = E_{\text{GGA}}(c, a) + \Delta(c, a) - \Delta(\infty, a)$ .
- [19] E. Ziambaras and E. Schröder, cond-mat/0304075.

\* To whom correspondence should be addressed; E-mail: lundqvist@fy.chalmers.se.

[1] J. P. Perdew, et al., Phys. Rev. B **46**, 6671 (1992); **48**, 4978(E) (1993).

- [20] The value of 33 GPa reported earlier [22] was incorrect.
- [21] M. V. Bollinger et al, Phys. Rev. Lett. **87**, 196803 (2001); M. V. Bollinger, K. W. Jacobsen, and J. K. Nørskov, Phys. Rev. B **67**, 085410 (2003).
- [22] H. Rydberg, et al., Surf. Sci., in print (2003).
- [23] *Landolt-Börnstein search* (Springer, Berlin, 2003), <http://link.springer.de>.
- [24] G. Kern, G. Kresse, and J. Hafner, Phys. Rev. B **59**, 8551 (1999).
- [25] Th. Böker et al., Phys. Rev. B **64**, 235305 (2001).
- [26] Y. Baskin and L. Mayer, Phys. Rev. **100**, 544 (1955).
- [27] L. X. Benedict *et al.*, Chem. Phys. Lett. **286**, 490 (1998).